# Non-linear dynamics of opto-thermally excited atomically thin graphene resonators

Robin J. Dolleman*, Farbod Alijani**, Herre S.J. van der Zant* and Peter G. Steeneken*,**
**Kavli Institute of Nanoscience, Delft University of Technology, Lorentzweg 1, 2628CJ Delft, The Netherlands*
***Department of Precision and Microsystems Engineering, Delft University of Technology, Mekelweg 2, 2628 CD Delft, The Netherlands*

*Summary*. We study the non-linear dynamics of suspended graphene membranes subjected to opto-thermal actuation. The periodic heating by the optical drive causes parametric resonance. A numerical model was developed following a Lagrangian approach and it is found that the presence of imperfections in the membrane causes direct and parametric resonances. The parametric resonance observed here provides an interesting outlook to study the coupling between mechanics and thermal properties of graphene with high accuracy.

## Introduction

Graphene is an extremely flexible material with an exceptionally high Young's modulus [1]. Due to geometric non-linearities, the tension in circular graphene membranes is strongly amplitude dependent [2], which makes graphene drums ideal model systems for studying the non-linear mechanics of nanomembranes. Although these Duffing nonlinearities have been observed in numerous works, the response of a graphene membrane to parametric excitation has received little attention. Here, we show that the opto-thermal actuation also gives rise to parametric excitation in graphene membranes. Interestingly even in a homodyne detection scheme a response to subharmonic excitation is observed, the cause of this effect is currently unknown.

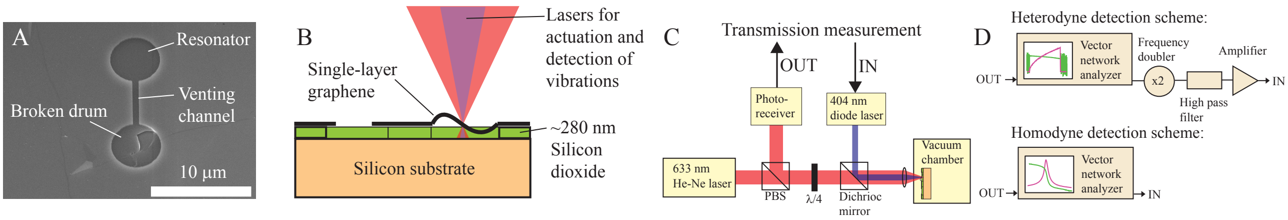


Figure 1: A: Scanning electron microscopy image of a single-layer graphene resonator; the top part forms the resonator and the bottom part is broken, forming a venting channel to the environment. B: Cross section of a device along the dumbbell length, showing the red and blue lasers that are used for readout and actuation of the vibration. C: Schematic of the interferometric setup used to actuate and read out the membrane motion. D: Schematic of the heterodyne detection scheme to detect parametric resonance and the homodyne detection scheme.

## Experimental setup and fabrication

Graphene drums are fabricated on a 280 nm layer of silicon dioxide in which dumbbell shaped cavities are etched. Graphene grown by chemical vapour deposition is transferred over the chip with a protective polymer on top. This polymer is dissolved and the sample is subsequently dried using critical point drying. During the drying process, one of the graphene drums in the dumbbell is broken by capillary forces. This is favorable, since it avoids the presence of trapped gas in the cavity below the graphene membrane that could cause pressure gradients across the membrane when evacuating the vacuum chamber. An example of a successful device is shown in Fig. 1A.

Figure 1B shows a cross-section of the resonator. The silicon substrate acts as a back mirror and the graphene acts as a moving mirror, creating a low-finesse Fabry-Perot cavity. A red He-Ne laser reads out the motion of the membrane and a modulated blue laser provides the actuation by thermal expansion of the membrane. Optical isolation components are used (Fig. 1C) to separate the blue and red laser in the setup. The measurement is performed by monitoring the electrical transmission $V_{\mathrm{OUT}}/V_{\mathrm{IN}}$ between the modulated blue laser and the interference detected by the red laser using a vector network analyzer (VNA).

## Experimental results

To detect parametric resonance a heterodyne detection scheme was employed (Fig. 1D). A frequency doubler was placed after the output port of the VNA and an amplifier was used to compensate the conversion losses. Figure 2A shows the magnitude and phase of the detected signal at different driving powers. The magnitude is well described by a square-root dependence on frequency and two stable phases are detected, which is consistent with parametrically driven resonators [3].

Figure 3A shows frequency responses of 4 different resonators with a diameter of 7 $\mu$m. In each resonator multiple of subharmonic and superharmonic responses are detected. Primary excitations of the fundamental resonance modes are labeled f' and in all cases the subharmonic is found at frequency 2f'. In addition, small superharmonic responses can be seen at frequency f'/2.

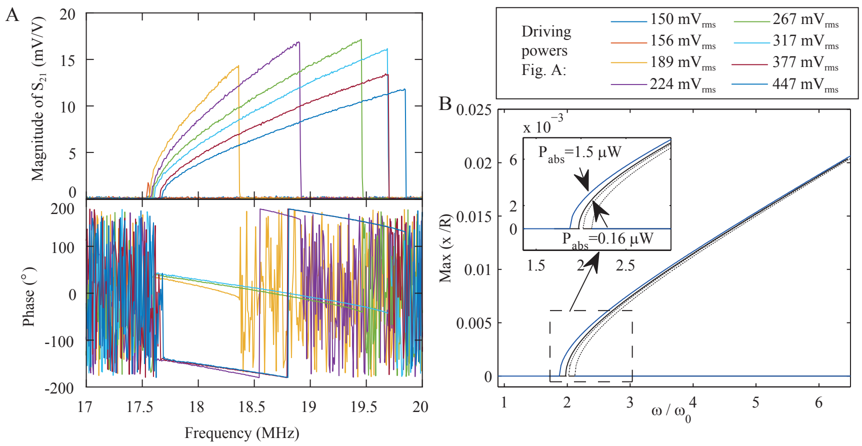

Figure 2: Graphene resonator parametrically driven by opto-thermal actuation in a heterodyne detection scheme. The frequency at the output port of the VNA was doubled in frequency, the frequency shown here is the frequency of the analyzer port. A: Measured magnitude of transmission and phase as function of frequency (forward sweep). B: Simulated parametric resonance (using eq. 1) of single-layer graphene membrane subjected to different absorption power.

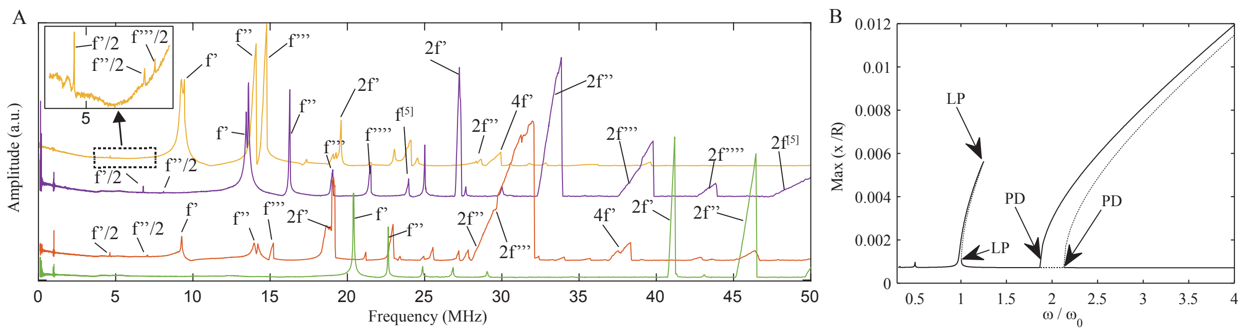

Figure 3: A: Measured response ($V_{\mathrm{OUT}}/V_{\mathrm{IN}}$) of the motion as a function of frequency for 4 different graphene drums with a diameter of 7 $\mu$m driven at 223.6 mV$_{\mathrm{rms}}$ in a homodyne detection scheme. B: Simulated non-linear response using eq. 1 of single-layer graphene membrane showing combined direct and parametric excitation due to the presence of imperfection. PD and LP denote period doubling and limit point bifurcations, respectively.

## Numerical model

A numerical model of the fixed graphene membrane is obtained by using a Lagrangian approach. This yields a system of non-linear ordinary differential equations with quadratic and cubic non-linear terms as follows:

$$\mathbf{M}\ddot{\mathbf{q}} + \mathbf{C}\dot{\mathbf{q}} + \Big[\mathbf{K1} + \mathbf{K2}\cos(\omega t) + \mathbf{N2(q)} + \mathbf{N3(q,q)}\Big]\mathbf{q} = \mathbf{f}\ \cos(\omega t), \tag{1}$$

where **M** is the mass matrix and **C** is the viscous damping matrix added to the equations of motion to introduce dissipation. Moreover, **K1** is the linear stiffness matrix dominated by the tension, **K2** is the coefficient of the time varying stiffness causing parametric excitation via optical power induced temperature variation in the membrane. Furthermore, **N2** gives the quadratic non-linear stiffness terms due to imperfection, **N3** denotes the cubic non-linear stiffness terms and **f** is the vector of direct external excitation due to the presence of imperfection. Indeed for a completely flat membrane, $\mathbf{N2} = \mathbf{f} = \mathbf{0}$. Next, a pseudo arclength continuation and collocation technique is used to detect bifurcations and obtain periodic solutions. Figure 2B shows the simulated parametric resonance of a single layer graphene drum for different levels of absorbed laser power ($P_{abs}$). This shows that the parametric response could be used to determine (opto-)thermal properties of graphene. Figure 3B shows combined primary and secondary resonances for the same membrane when it is initially deviated from flat configuration. The deviation causes simultaneous direct and parametric resonance of the membrane which might account for the secondary resonances observed in Fig. 3A.

## Acknowledgments

We thank the Dutch Technology Foundation (STW) and the European Union's Horizon 2020 research and innovation programme under grant agreement No 649953 Graphene Flagship for financially supporting this work.

## References

[1] Lee, Changgu, et al. "Measurement of the elastic properties and intrinsic strength of monolayer graphene." Science 321.5887 (2008): 385-388.

[2] Eichler, A., et al. "Nonlinear damping in mechanical resonators made from carbon nanotubes and graphene." Nature nanotechnology 6.6 (2011): 339-342.

[3] Mahboob, I., et al. "A multimode electromechanical parametric resonator array." Scientific reports 4 (2014): 4448.